ICAS-82-2.6.4

DESIGN AND FABRICATION OF COCURED COMPOSITE HAT-STIFFENED PANELS

G.D. Peddie* and E.E. Spier‡

General Dynamics Convair Division
P.O. Box 80847, MZ 55-4700
San Diego, California 92138

Abstract

Design/analysis study established cocured graphite-epoxy hat-stiffened panels of high compressive structural integrity for development and demonstration by mechanized methods. Both flat and curved-crown hats were involved in the design/analysis study, but only the flat-crown concept was included in the manufacturing study. It was found that manufacture of the curved-crown hat would not result in added complexity. Post-buckling structural integrity was assumed to be directly related to the summation of classical local bifurcation buckling strengths of panel elements. Parts were built in stages with the final panel being 18 feet long. Mechanization and tooling procedures were proven to be valid for the manufacture of long panels. Test panels were not fabricated in time for correlation with analysis, but testing will be performed in the near future.

Nomenclature

A	area
$\overline{A}$	total cross-sectional area† (see Eq. 4)
E_L^c	longitudinal compressive modulus of elasticity
E_T^t	transverse tensile modulus of elasticity
F^{cy}	yield strength
G_{LT}	in-plane shear modulus of rigidity
K	efficiency factor, $10^{-4}P/\overline{A}$
$\overline{K}$	efficiency factor, $10^{-5}\,\overline{P}/\overline{A}$
n	exponent in Eq. 1
P	summation of classical bifurcation buckling loads (P_{cl}^{cr}) for branches 3 and 5 (total cross-section)†
$\overline{P}$	summation of classical bifurcation buckling loads (P_{cl}^{cr}) for branches 3, 4 and 5 (total cross-section)†
P_{cl}^{cr}	classical bifurcation buckling load
T/C	thermocouple
v/o	fiber percent by volume
x_g, y_g, z_g	global coordinates
X,Y,Z	local coordinates
α	angle of hat-section web (Figs. 1 and 3)
α_1	coefficient in Eq. 1
θ	lamina angle with respect to 0(X)-direction
ν_{LT}	major Poisson's ratio
σ^{cr}	buckling stress
σ^{cc}	postbuckling (crippling) stress

† Total cross-section values are equal to twice those for the STAGSC symmetric half-model.

* Senior Manufacturing Engineer.

‡ Engineering Specialist; member AIAA.

I. Introduction

The near-term introduction of composite materials in aircraft and missile primary structures is driven by growing demands for increased energy efficiency, improved performance, or both. The specific strength and stiffness of composites far exceed corresponding properties for metals. When properly applied, composites yield significant weight savings that translate into reduced fuel consumption, greater range, higher speed, and overall vehicle downsizing to reflect reduced fuel requirements. However, piece-wise substitution of composites for corresponding metal parts has been the predominant approach in most but, fortunately, not all recent applications. This approach, though technically acceptable, is costly in fabrication and does not maximize the performance payoff. Mechanized manufacturing methods offer solid potential to produce integrated composite structures with reduced parts count, lower manufacturing labor costs, and considerable weight reduction. The trend is toward cocuring and mechanization, but this area of activity, though widely recognized, is still in its infancy, especially in the case of large, stiffened structures. Cost-effective manufacturing techniques for the fabrication of efficient, integrally stiffened composite structures for both military and commercial aircraft and missiles are needed. Accordingly, this paper is concerned with design/analysis and manufacturing approaches to fabricating cocured, hat-stiffened evaluation panels. The design concepts (Figs. 1 and 2) are representative of both wing and fuselage aircraft structures and are the baseline compression components considered in the present study.

The composite material selected for analysis was T-300/5208 tape. Evaluation of woven cloth has been deferred to a later time. The 0.040-inch skin stacking sequence was $[\pm 45/0/90]_S$ in all cases. A selected laminate for the crown of the hat continues down the webs until half of the laminate turns outward and becomes part of the flange; the other half is turned inward and overlaps as shown in (Figs. 1 and 2) so that this element behaves in compression at least as well as a conventional plate element. These configurations provide the highest compressive structural integrity possible for the hat-section concepts investigated. Components of the design concepts will be fabricated and tested in the near future for determination of ulitimate local postbuckling compressive strength. Then, the test data will be compared to the analysis results and evaluated.

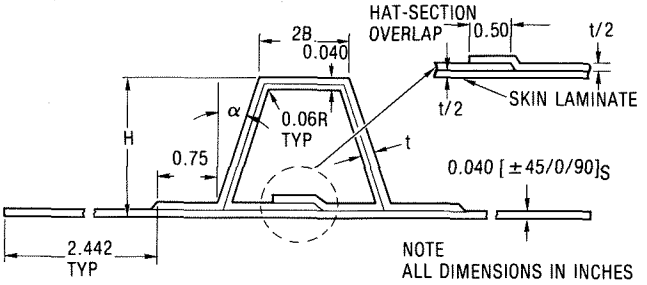

Fig. 1 Cocured flat-crown, hat-stiffened panel cross-section.

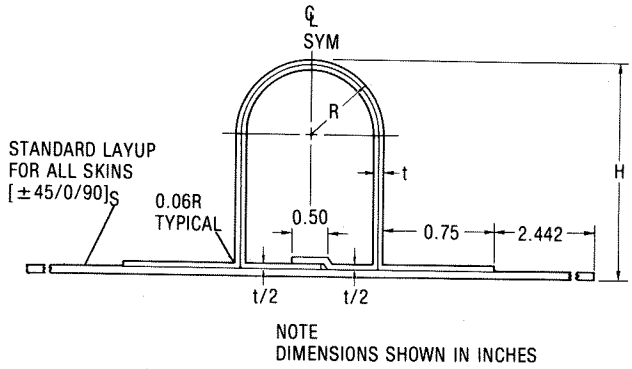

Fig. 2 Cocured curved-crown, hat-stiffened panel cross-section.

II. Design and Analysis

Theoretical methods for reliable prediction of the ultimate compressive postbuckling strength of the composite hat-stiffened panels shown in Figs. 1 and 2 are not currently within the state of the art. Accordingly, semiempirical techniques[1-3] offer the most promise at this time. Evaluation and screening of design concepts resulted in selection of a set of highly efficient hat-stiffened panels to manufacture and subsequently test. It has been shown by Gerard[4] that the postbuckling (crippling) strength of a metal plate is a function of the buckling strength according to the following expression:

$$\frac{\sigma^{cc}}{F^{cy}} = \alpha_1 (\sigma^{cr}/F^{cy})^{1-n} \tag{1}$$

For expediency, bifurcation buckling analysis by use of the STAGSC computer code[5] was used to obtain qualitative loads and efficiencies between design concepts rather than quantitatively correct loads. The material used for the analysis was T-300/5208 tape, where the mechanical properties for 64 percent v/o were

$$E_L^c = 21.8 \times 10^6 \text{ psi} \qquad E_T^t = 1.4 \times 10^6 \text{ psi}$$

$$G_{LT} = 0.74 \times 10^6 \text{ psi} \qquad \nu_{LT} = 0.3$$

A symmetrical half-model for analysis of the flat-crown hat (Fig. 1) is shown in Fig. 3, which is divided into five branches, as shown, to satisfy the computer code requirements. The stacking sequence of the skin is held constant at $[\pm 45/0/90]_S$ with a width of 2.442-inches in all cases. Also, the overall height is maintained at 1.22-inches, and the flange width is held at 0.75-inch. Thus, the design variables are the dimension (B), the angle (α), and the stacking sequences of branches 2-5. The computer code requires a finite-difference model which is shown in Fig. 4. The global (x_g, y_g, z_g) and local (X,Y,Z) coordinate systems are shown. The mesh points in the cross-section lie along equally spaced imaginary lines in the Y-direction. These lines are referred to as columns and run parallel to the X-direction. Corresponding lines, equally spaced in the X-direction, are known as rows and run parallel to the Y-direction. The rows and/or columns do not have to be equally spaced, but sufficient numbers must be provided to obtain valid bifurcation buckling loads. Minimizing the number of rows and columns keeps the computer costs at a minimum.

It is convenient to obtain the local bifurcation buckling loads for each branch by separate computer runs, where all other branches are linearized, thereby simulating instability suppression in all but one branch. This results in overly optimistic in-plane boundary conditions for the buckled element. Also, an element with an adjacent buckled element is always "triggered" into out-of-plane displacements so that the deformations are compatible.[6,7] The net result is that calculated buckling loads for each branch are extremely optimistic but qualitatively comparable. Since the plate elements of the hat may be considered narrow, the buckling loads are further optimistic[1]. Because of these several influences, the sum of the calculated buckling loads for the branches are much higher than the crippling strengths. Nevertheless, the calculated buckling loads obtained in this manner do provide qualitative comparisons of probable crippling strengths between the design cases considered.

For an initial qualitative analysis of the hat-stiffened panel (Fig. 1) for comparative evaluations between design cases, it is convenient to express index parameters in the form

$$P = P_{cl}^{cr} \text{ (branch 3)} + P_{cl}^{cr} \text{ (branch 5)} \tag{2}$$

$$K = 10^{-4} P/\overline{A} \tag{3}$$

where

$$\overline{A} = \sum_{2}^{5} A \text{ (branch)} \tag{4}$$

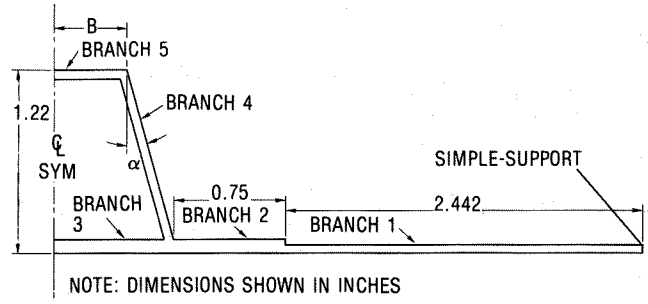

Fig. 3. Half-model for flat-crown hat-stiffened panel.

Branch 4 would also logically be included for P, but was omitted to reduce computer costs. Branch 2 was purposely omitted from P because its buckling strength would be "triggered" early by the low buckling strength of Branch 1 (also omitted). It will be shown later that inclusion of Branch 4 for the curved-crown concept (Fig. 2) substantiated identical conclusions to those obtained for the flat-crown concept. The index value for K represents an efficiency factor of allowable load to cross-sectional area (or load to weight ratio) of the hat-stiffened panel shown in Fig. 1. The results of a limited comparative analysis for many design cases are shown in Table 1. These data are also shown plotted in Fig. 5 with K versus P. Some definite conclusions may be stated by inspection of Table 1 and Fig. 5 as follows:

1. The structural efficiency of a panel increases as the value for α decreases as shown in Fig. 6.
2. Ninety-degree plies at the midsurface are far more efficient than zero-degree plies. This is to be expected because 90-degree plies provide superior boundary conditions to adjacent elements in resisting out-of-plane displacements. Compare panels 1, 2 and 3 in Table 1, Fig. 5, and Fig. 6.
3. The removal of any plies form branch 4 will reduce the structural efficiency of the panel. Compare panels 1, 1-A, 1-B, and 1-C; 2, 2-A, 2-B, and 2-C; and 3, 3-A, 3-B, and 3-C.
4. Modules of $[\pm 75]_S$ plies may be substituted for $[90]_4$ plies at the mid-surface without appreciable loss of efficiency. Compare panel 4 with 1 and 4R-A with 1R-C.

To finalize the study and also include the curved-crown concept, the design cases were limited to those with α = 0-degrees. These includes ID = IR-B and those in Fig. 5 with both higher K and P values: ID = IR-C, IR-D, IR-F, IR-G, 2R-A and 2R-B. Concept 4R-A was not included because the results would be nearly identical to 1R-C, and 1R-E was arbitrarily excluded. The symmetrical half-model employed for analysis of the curved-crown hat (Fig. 2) is shown in Fig. 7. The value for H was derived

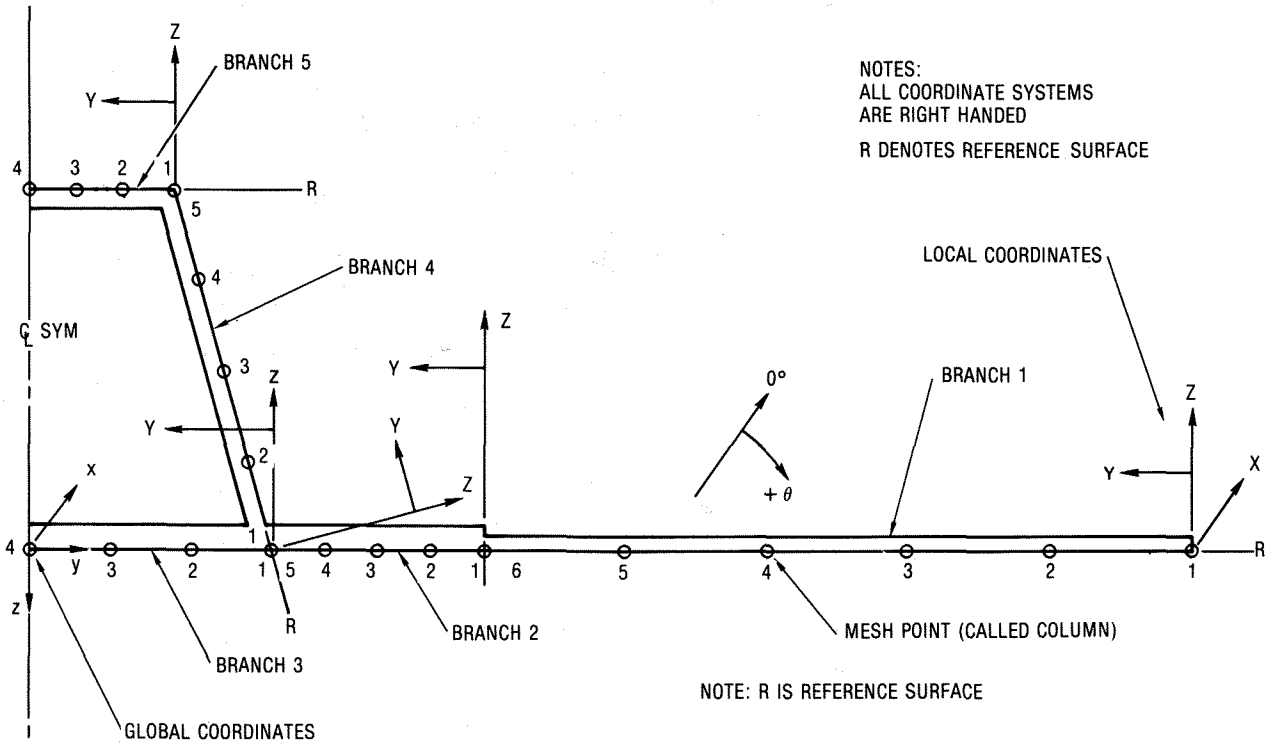

Fig. 4 Finite-difference half-model for flat-crown hat-stiffened panel.

Table 1 Configuration and analysis results of flat-crown hat-stiffened panels.

			BRANCH 5			BRANCH 4				
ID	B (IN.)	α (DEG)	STACKING SEQUENCE	NO. PLIES	t (IN.)	STACKING SEQUENCE	NO. PLIES	t (IN.)	P (KIPS)	K (LB/IN.^{2})
1	0.5	15	$[\pm 45/0_2/90_2]_S$	12	0.060	$[\pm 45/0_2/90_2]_S$	12	0.060	28.95	6.87
1-A	0.5	15	↓	↓	↓	$[\pm 45/0_2/90]_S$	10	0.050	24.59	6.44
1-B	0.5	15	↓	↓	↓	$[\pm 45/0_2/\overline{90}]_S$	9	0.045	21.93	6.19
1-C	0.5	15	↓	↓	↓	$[\pm 45/0/90]_S$	8	0.040	19.87	5.81
1R-A	0.5	7.5	↓	↓	↓	$[\pm 45/0_2/90_2]_S$	12	0.060	32.51	8.18
1R-B	0.5	0	↓	↓	↓	$[\pm 45/0_2/90_2]_S$	12	0.060	38.12	10.42
1R-C	0.5	0	$[\pm 45/0_2/90_3]_S$	14	0.070	$[\pm 45/0_2/90_3]_S$	14	0.070	51.27	12.43
IR-D	0.6	0	$[\pm 45/0_2/90_4]_S$	16	0.080	$[\pm 45/0_2/90_4]_S$	16	0.080	58.70	11.88
IR-E	0.8	0	$[\pm 45/0_2/90_6]_S$	20	0.100	$[\pm 45/0_2/90_6]_S$	20	0.100	70.01	10.25
IR-F	0.7	0	$[\pm 45/0_2/90_6]_S$	20	0.100	$[\pm 45/0_2/90_6]_S$	20	0.100	82.34	12.68
IR-G	0.7	0	$[\pm 45/0_2/90_5]_S$	18	0.090	$[\pm 45/0_2/90_5]_S$	18	0.090	63.86	10.78
2	0.5	15	$[\pm 45/0_3/90]_S$	12	0.060	$[\pm 45/0_3/90]_S$	12	0.060	27.56	6.55
2-A	0.5	15	↓	↓	↓	$[\pm 45/0_2/90]_S$	10	0.050	23.50	6.16
2-B	0.5	15	↓	↓	↓	$[\pm 45/0_2/\overline{90}]_S$	9	0.045	21.80	6.15
2-C	0.5	15	↓	↓	↓	$[\pm 45/0/90]_S$	8	0.040	19.77	5.78
2R-A	0.5	0	$[\pm 45/0_3/90_2]_S$	14	0.070	$[\pm 45/0_3/90_2]_S$	14	0.070	47.75	11.57
2R-B	0.6	0	$[\pm 45/0_3/90_3]_S$	16	0.080	$[\pm 45/0_3/90_3]_S$	16	0.080	56.81	11.49
3	0.5	15	$[\pm 45/0_4]_S$	12	0.060	$[\pm 45/0_4]_S$	12	0.060	24.18	5.74
3-A	0.5	15	↓	↓	↓	$[\pm 45/0_3]_S$	10	0.050	18.76	5.48
3-B	0.5	15	↓	↓	↓	$[\pm 45/0_2]_S$	8	0.040	15.79	5.21
4	0.5	15	$[\pm 45/0_2/\pm 75]_S$	↓	↓	$[\pm 45/0_2/\pm 75]_S$	12	0.060	28.73	6.82
4R-A	0.5	0	$[\pm 45/0_2/\pm 75/90]_S$	14	0.070	$[\pm 45/0_2/\pm 75/90]_S$	14	0.070	51.38	12.44

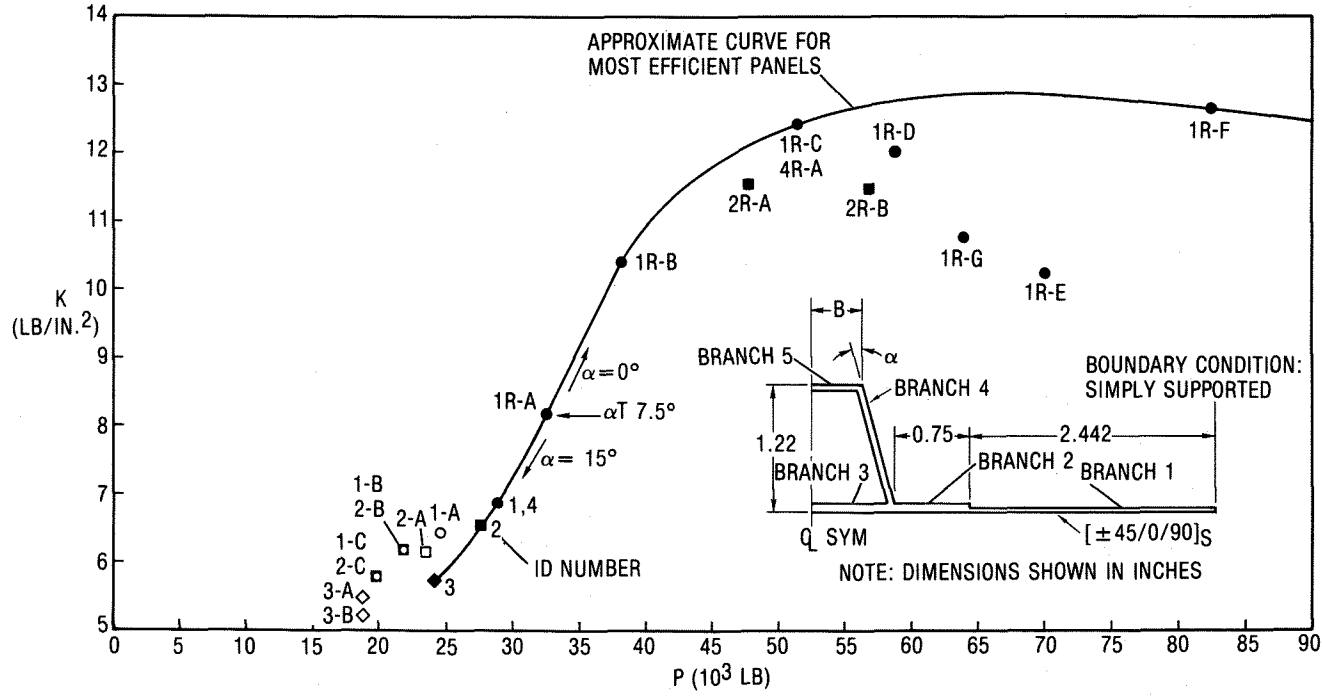

Fig. 5 Efficiency versus load plot for flat-crown hat-stiffened panels.

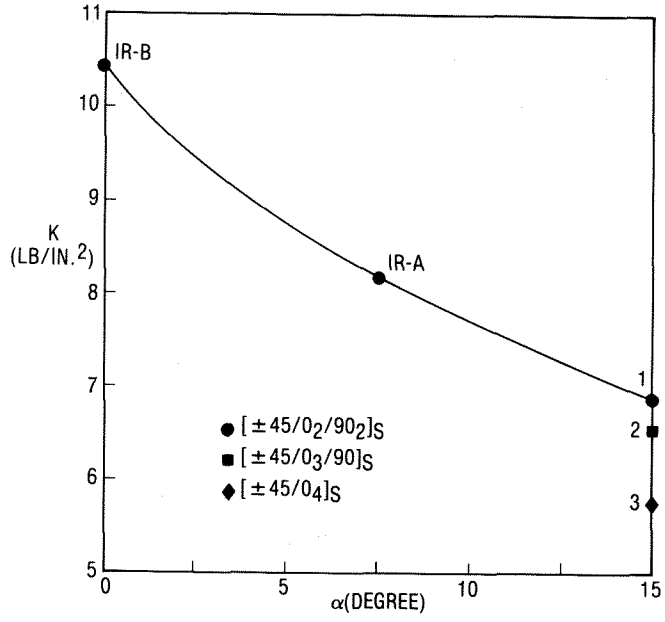

Fig. 6 Effect of angle (α) on efficiency factor (K).

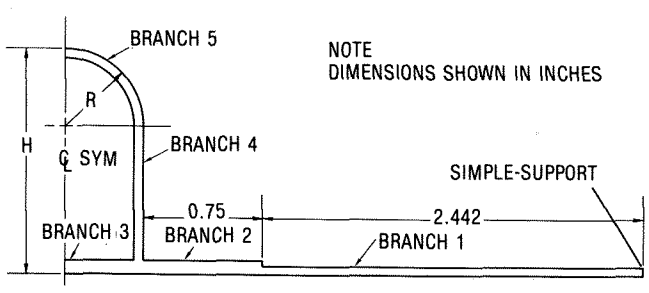

Fig. 7 Half-model for flat-crown hat-stiffened panel.

for equivalency of the hat perimeters; i.e., the sum of the developed lengths of branches 4 and 5 were made equal for both design concepts (Figs. 3 and 7). The cross-sectional areas were also approximately equivalent. Other constraints remained the same, and the value for R was made equal to B. The STAGSC finite-difference model is shown in Fig. 8.

In this final phase of the investigation the analysis approach was expanded to recognize the critical load contribution from the hat webs (branch 4). The index parameters (Eqs. 2 and 3) were therefore redefined as follows:

$$\overline{P} = \sum_{3}^{5} P_{cl}^{cr}\,(\text{branch}) \tag{5}$$

$$\overline{K} = 10^{-5}\ \overline{P}/\overline{A} \tag{6}$$

The results of the buckling analysis are shown in Table 2 and Fig. 9, where ID = 1R-B is used as a reference baseline to establish index points; thus $K/K_{1R\text{-}B}$ is plotted versus $\overline{P}/\overline{P}_{1R\text{-}B}$. Notice that ID = 1R-$B_a$, 1R-$B_b$, 1R-$B_c$ and 1R-B_b/C all have some plies in branch 4 removed; and, as before, this becomes detrimental to the efficiency of the panels. Notice that ID = 1R-B_a has $[\pm 45/90]_S$ plies in branch 4, which is superior to the $[\pm 45/0]_S$ plies in branch 4 of ID = 1R-B_b. Thus it has again been shown that 90-degree plies are superior to 0-degree plies at the midsurface. It is quite obvious that the curved-crown concept is much more efficient than the flat-crown concept. Observe in Fig. 9 that the paths of the index points are nearly linear for both the flat and curved-crown concepts. The index points for the concepts with plies removed from branch 4 deviate from this linearity; notice that the curved-crown concept ID = 1R-B_b/C demonstrates just a modest improvement over ID = 1R-B. Analysis of curved-crown cases was extended to include the effect of height (H) variations. Accordingly, the results for three different values for H (1.23, 1.43 and 2.03-inch) are shown in Fig. 10 for all cases except those with plies removed from branch 4. As expected, the local buckling strengths become less for an increase in H. This is generally the case because the wider width of branch 4 results in lower buckling strength for branch 4 and reduced boundary support to branches 3 and 5. When Euler-type buck-

Table 2. Configuration and analysis results of flat and curved- crown hat-stiffened panels.

SYMBOL	ID	B (IN.)	R (IN.)	H (IN.)	BRANCH 5		BRANCH 4		$\bar{P}$	$\bar{K}$
					STACKING SEQUENCE	NO. PILES	STACKING SEQUENCE	NO. PILES	(KIPS)	(LB/IN^2)
○	1R-B	0.5		1.22	$[\pm 45/0_2/90_2]_s$	12	SAME AS BRANCH 5	12	71.99	1.97
⊕	1R-B_a	0.5		1.22	$[\pm 45/0_2/90_2]_s$	12	$[\pm 45/90]_s$	6	49.91	1.66
◒	1R-B_b	0.5		1.22	$[\pm 45/0_2/90_2]_s$	12	$[\pm 45/0]_s$	6	44.83	1.49
◐	1R-B_c	0.5		1.22	$[\pm 45/0_2/90_2]_s$	12	$[\pm 45]_s$	4	40.98	1.47
○C	1R-B/C		0.5	1.43	$[\pm 45/0_2/90_2]_s$	12	SAME AS BRANCH 5	12	112.17	3.13
◒C	1R-B_b/C		0.5	1.43	$[\pm 45/0_2/90_2]_s$	12	$[\pm 45/0]_s$	6	73.43	2.32
●	1R-C	0.5		1.22	$[\pm 45/0_2/90_3]_s$	14	SAME AS BRANCH 5	14	105.48	2.59
●C	1R-C/C		0.5	1.43	$[\pm 45/0_2/90_3]_s$	14	SAME AS BRANCH 5	14	158.28	3.78
□	1R-D	0.6		1.22	$[\pm 45/0_2/90_4]_s$	16	SAME AS BRANCH 5	16	131.60	2.73
□C	1R-D/C		0.6	1.48	$[\pm 45/0_2/90_4]_s$	16	SAME AS BRANCH 5	16	194.80	3.94
◪	1R-G	0.7		1.22	$[\pm 45/0_2/90_5]_s$	18	SAME AS BRANCH 5	18	163.72	2.92
◪C	1R-G/C		0.7	1.52	$[\pm 45/0_2/90_5]_s$	18	SAME AS BRANCH 5	18	239.53	4.15
■	1R-F	0.7		1.22	$[\pm 45/0_2/90_6]_s$	20	SAME AS BRANCH 5	20	190.81	3.14
■C	1R-F/C		0.7	1.52	$[\pm 45/0_2/90_6]_s$	20	SAME AS BRANCH 5	20	305.03	4.86
◇	2R-A	0.5		1.22	$[\pm 45/0_3/90_2]_s$	14	SAME AS BRANCH 5	14	101.34	2.47
◇C	2R-A/C		0.5	1.43	$[\pm 45/0_3/90_2]_s$	14	SAME AS BRANCH 5	14	152.00	3.55
◆	2R-B	0.6		1.22	$[\pm 45/0_3/90_3]_s$	16	SAME AS BRANCH 5	16	126.92	2.77
◆C	2R-B/C		0.6	1.48	$[\pm 45/0_3/90_3]_s$	16	SAME AS BRANCH 5	16	187.97	3.79

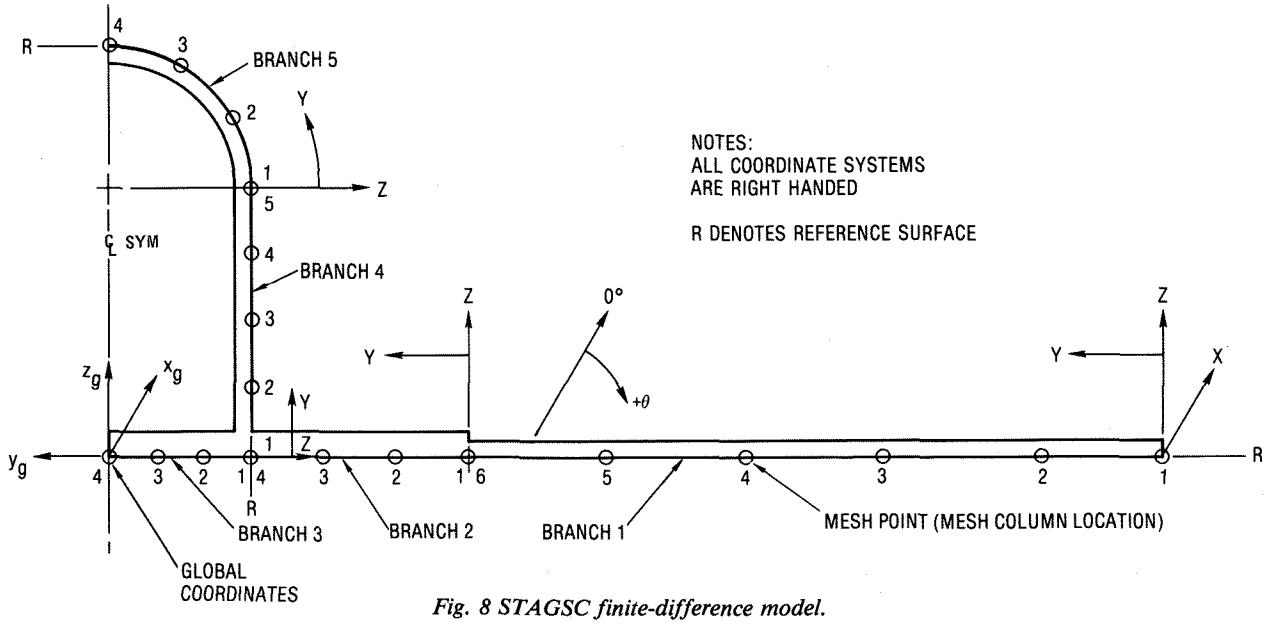

Fig. 8 STAGSC finite-difference model.

ling becomes more dominant as the length of the panel increases, the trend may tend to reverse; then the buckling load could increase for a higher value for H.

III. Manufacturing

Current Composite Manufacturing State of The Art

Significant cost-effective manufacturing techniques for the fabrication of efficient, large, integrally stiffened composite structure for both military and commercial aircraft and missiles are lacking. However, aircraft and missile structures can be manufactured using advanced composite materials and composite manufacturing processes can be cost-effective and competitive compared to aluminum fabrication methods if mechanized.

Manufacturing Objective

The manufacturing objective was the development of compatible design approaches and manufacturing techniques for cost-effective manufacture of efficient stiffened composite structures through the coordinated evaluation of mechanized fabrication concepts and improved layup technology. That objective was oriented toward heat and pressure cocuring of multiple subelements into complete, integrally stiffened panels representative of typical commercial and military aircraft structures. The emphasis was placed on the elimination of major hand-layup operations in order to reduce cost while increasing the quality and production rate of large component structures.

Component Selection

Early in the manufacturing study, many aircraft design and fabrication documents were studied. These suggested a myriad of study possibilities. Work performed by many companies and General Dynamics Convair Division proposals were reviewed for possible structural candidates for analysis and manufacturing development work. The initial baseline structural component selected for study was a flat-crown hat-stiffened panel. Toward the end of the 1981 study, a curved-crown concept was proven to

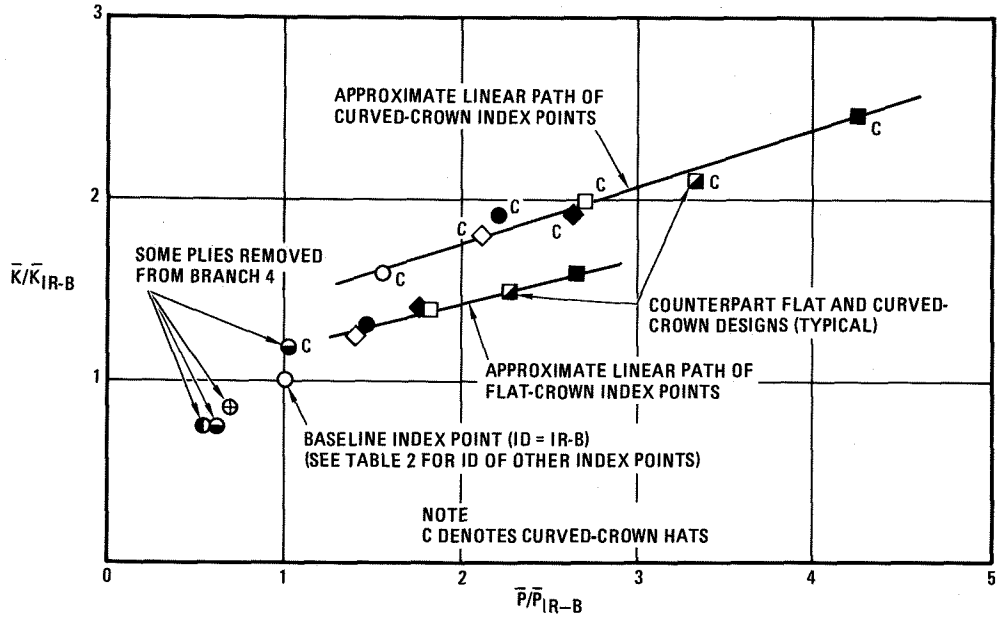

Fig. 9 Nondimensional index points for hat-stiffened panels.

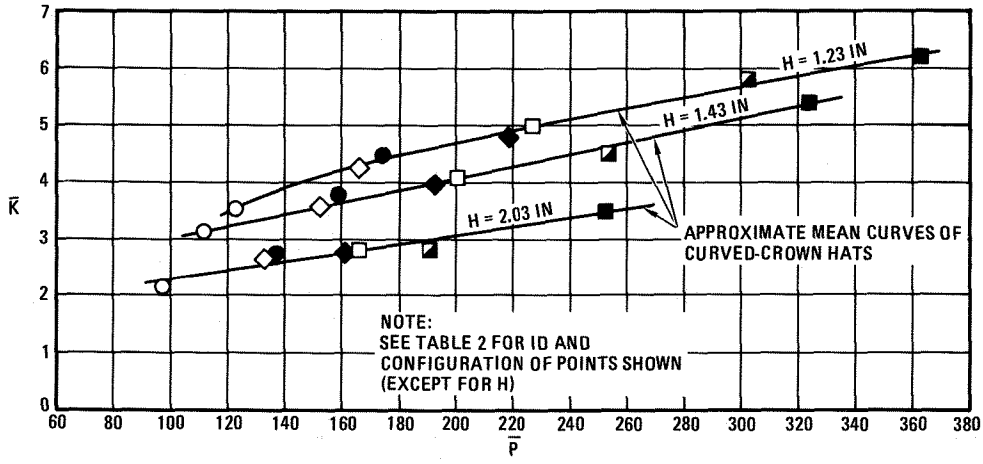

Fig. 10 Effect of height (H) on $\bar{K}$ versus $\bar{P}$ for curved-crown hat-stiffened panels.

be much more efficient. This design will be addressed subsequently. The first selected concept is shown in Fig. 11. It was selected because of its common use in aerospace wing, fin, and fuselage structures. The cross-section is shown in detail in Fig. 12. It incorporated angle (α), height, and width derived from various designs shown in the literature.

In the baseline design concept, a web angle of $\alpha = 30$ degrees was employed in both four-inch and 18-inch development parts prior to initiating the detail design/analysis effort. The objective of this effort was to establish near-optimum shapes and ply stacking sequences before any work was started on an 18-foot long demonstration structure. A preliminary, but not optimum, design was developed in time for the work on the 18-foot long demonstration part. Further analysis did optimize the design as reported in Section II.

Material Selection

Weight and mechanical properties are among the most important considerations in the selection for a material for the fabrication of structurally efficient composite aerospace hardware; however, of equal importance are practical considerations such as:

1. Ease of fiber-ply layup.
2. Considerations of the thermal expansion differentials between the composite and tooling materials.
3. Availability of materials having reliable physical and chemical properties.

Initially, it was decided that all demonstration hardware would be fabricated primarily from woven graphite-epoxy materials rather than unidirectional fiber materials. The woven material selection was based on the following assumptions:

1. Woven fabric should be more adaptable for mechanized equipment layup process.
2. The hand layup process is also facilitated by the use of woven fabric. A design and manufacturing study directly comparing woven with unidirectional tape was initiated and is still in progress.

The selected material was Narmco Rigidite 5208-T300-42 plain-weave graphite-epoxy. The fabric was woven with 3,000 individual fibers per bundle (tow). The 5208 epoxy resin system was selected because of the extensive experience gained through the use of this material by industry. The impregnated material was

supplied with a resin content of 35 percent and a fiber weight of 193 gm/m^2. The woven fabric properties are:

$E^c = 9.4 \times 10^6$ psi
$E^t = 9.9 \times 10^6$ psi
$G = 1.0 \times 10^6$ psi
$\nu = 0.12$

} Average for warp and fill

Manufacturing Plans

Three successive manufacturing sequence plans were prepared in an evolutionary development with successive modification efforts aimed at removing some steps and consolidating others to reduce the total number of sequences in the manufacturing process. The first sequence plan had 14 main steps, while the last (number 3) shown in Fig. 13 had only eight main steps (circled), all of which could be readily modified for mechanization. The number 1 plan was used to fabricate four-inch parts, the 18-inch parts were fabricated to plan number 2, and plan number 3 was prepared for making the 18-foot component.

Tooling for the 4-inch Parts

All tooling was designed with mechanized layup of woven material as the primary objective. The tooling was also designed for existing production shop techniques to eliminate the possibility of new tooling developments adversely affecting normal fabrication method sequence evolution from preliminary concepts to near-optimum established processes. All hat-stiffened evaluation parts were fabricated using woven fabric. The fabric selected for the subscale development work was Style 181 plain-weave glass fabric impregnated with one of several production-type epoxy resins. The full-scale part used the Thornel T300 plain-weave graphite fabric impregnated with Narmco 5208 epoxy resin. The glass fabric for subscale development work was selected in order to start development work without the delays due to receipt of the long-lead time graphite fabric.

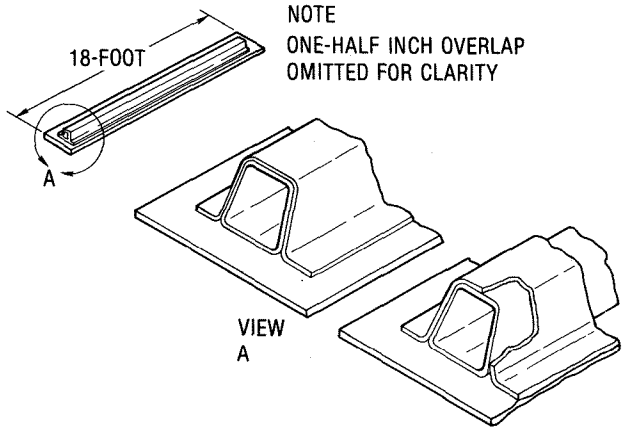

Fig. 11 Selected panel configuration.

Fig. 14 shows all of the inexpensive tools designed and made for fabricating four-inch long evaluation parts to validate the first manufacturing sequence plan before making larger parts. Only the steps in the manufacturing process were to be evaluated.

The tools were designed and made using formed and riveted sheet aluminum as well as wood. The cross-sections of the tools were full-scale; length was subscale. Tool (A) of Fig. 14 represents the hat-section forming and curing tool. This tool was used throughout the hat-section layup stages, and is considered the most important tool (with modifications) for use in a mechanized production fabrication processing tool. Tool (B) is the fabric ply forming block. Tool (C), although made of wood, represents an inflatable rubber mandrel tool. Tool (D) is the tool on which ten plies of fabric for the skin were layed up.

All of the tools for fabricating the four-inch parts were coated with a nonsilicone release agent (Frekote 44) prior to layup so as to ensure that the cured composite part would easily separate from the tools. All metal tools were baked for 30 minutes in a 350F oven to adhere the parting agent firmly to the tool surfaces. A second coating was wiped on after the tools had cooled to room temperature. Then, following a 15-minute air drying, the surfaces were lightly buffed with clean cheesecloth. All of the hardwood tools were sealed with lacquer sealer and air dried. Pressure-sensitive Teflon tape was then bonded to the wood surface to provide a permanent resin release system.

Fabrication of Four-Inch Parts

All hat-section plies for the four-inch parts were cut in accordance with the configuration shown in Fig. 12. Fig. 15 shows the wooden ply forming tool with all of the hat-stiffener plies in palce. Strips of Teflon-coated fabric (Armalon) were

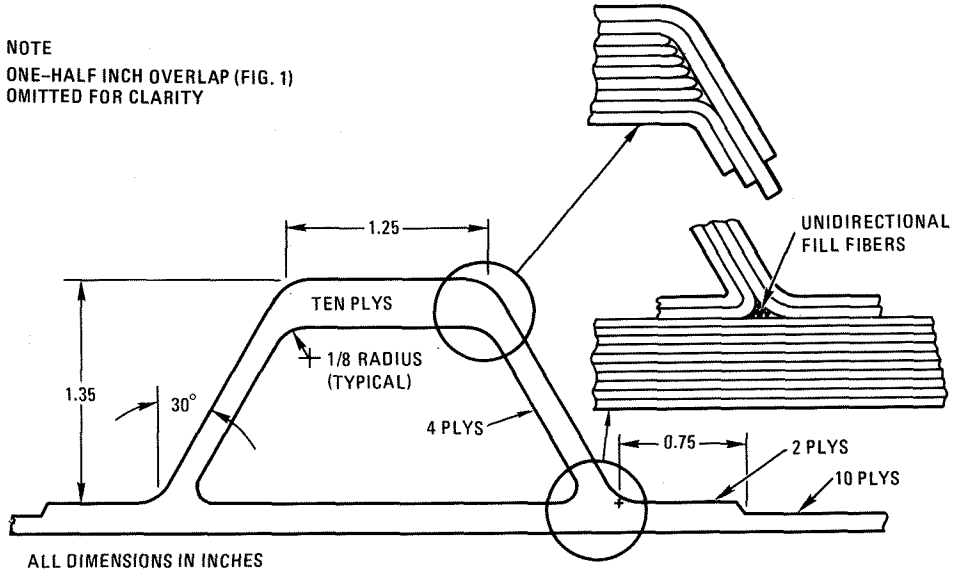

Fig. 12 Cross-section of panel configuration.

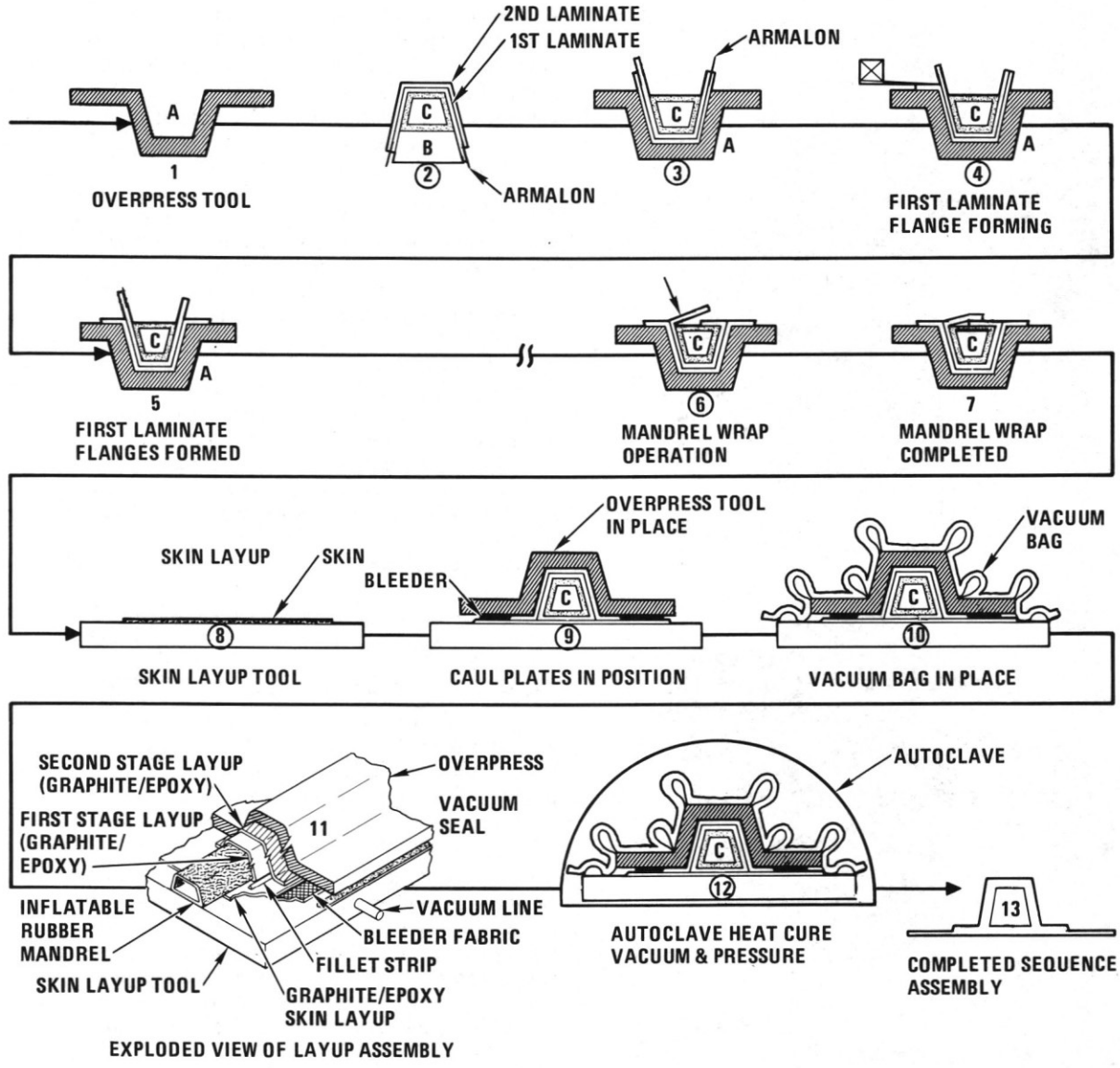

Fig. 13 Manufacturing sequence number 3.

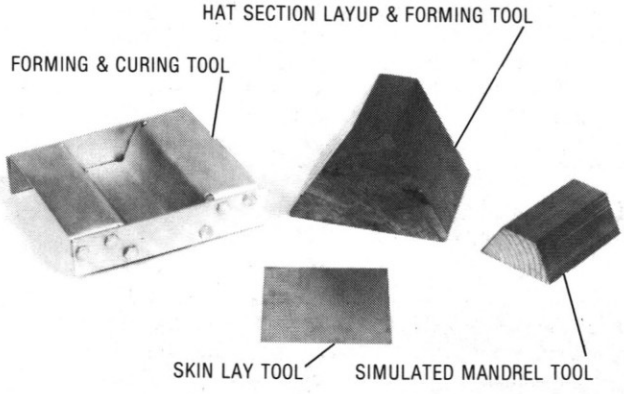

Fig. 14 Tools for fabrication of four-inch parts.

placed between the inboard and outboard flange area plies to provide a simple method for separating the flanges for forming. Fig. 16 shows the hat-stiffener tool in place in the aluminum forming and curing tool. The flange plies were tightly pressed against the forming and curing tool. The wooden mandrel was then placed in the hat-section layup, and the inboard flanges folded over the mandrel. The flat skin plies were then placed on the hat layup and the entire assembly envelope vacuum-bagged for a heat cure. The assembly was placed in a 275F oven. The total cure time at that temperature was three hours. The four-inch cocured evaluation part was then removed from the tools, and the wooden mandrel pulled out. Fig. 17 shows the finished four-inch long part.

The finished four-inch parts were evaluated with the intent of eliminating as many of the original manufacturing sequence steps as possible to reduce both labor and material costs prior to fabricating larger 18-inch parts. Changes to sequence number 1 were made and a second manufacturing sequence was prepared for the 18-inch part fabrication work. The information derived from the four-inch part fabrication work resulted in the elimination of four steps in the first fabrication sequence. This was accomplished by laying up all of the hat-section plies on the layup block in one operation. It was also determined that all constituents of the hat-stiffened layup could be formed easily by loosely stacking them together before forming rather than

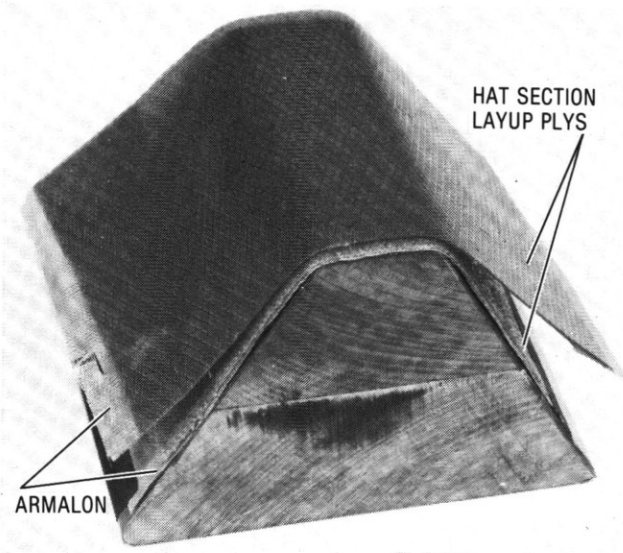

Fig. 15 Four-ply hat layup on hat-section layup tool.

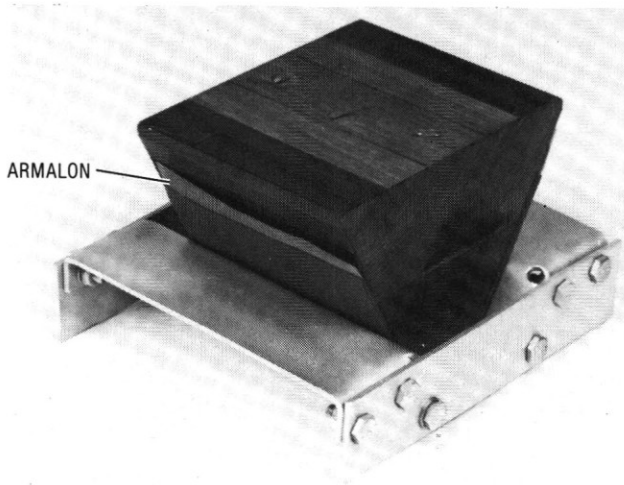

Fig. 16. Hat layup inserted in cocuring tool.

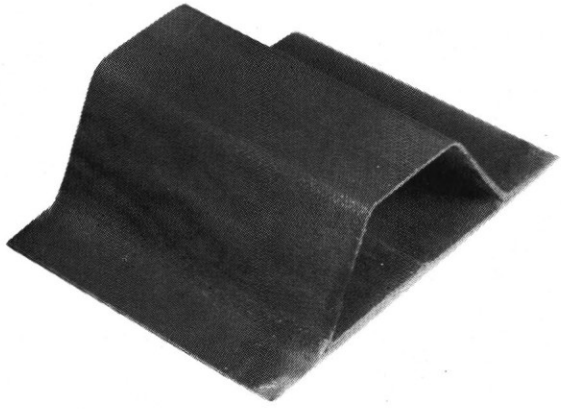

Fig. 17 Cocured hat-stiffened skin part.

precompacting them under full vacuum prior to forming. This system was more compatible with mechanical processing than individual preplying or precompacting.

Tooling and Tool Fabrication for 18-inch Long Parts

The rigid aluminum forming and curing tool used for the four-inch parts was replaced by the formed aluminum overpress tool shown in Fig. 18. It was decided that a more flexible tool was needed to allow the skin contour tool to be the dominant shape controlling tool, while the overpress tool is able to conform to the shape of the skin layup tool. This would be especially true with contoured skin configurations. The skin layup and curing tool was a flat ½-inch thick by 24-inch wide, by 36-inch long aluminum plate.

Fabrication of 18-Inch Parts

As with the 4-inch parts, all 18-inch evaluation parts were fabricated from woven glass fabric impregnated with a production epoxy system due to long lead-time considerations with the selected woven graphite material. The design shown in Fig. 12 (except for the removal of thick hat crown plies) was used in fabricating the 18-inch parts with a revised manufacturing plan (number 2). The wooden mandrel used in the four-inch development work was replaced by a hollow elastomeric rubber mandrel. A hollow rather than solid mandrel configuration was selected to control the internal pressures of the mandrel and also for ease of mandrel removal from the confining hat layup. One-eighth inch thick unruled silicone rubber sheet stock was selected as the starting material for the mandrels. The sheet stock was wrapped around an aluminum tool which was then placed in a closed mold for a heat cure under vacuum followed by a nonvacuum post cure. Fig. 19 shows the rubber mandrel ready for the hat-section layup.

Evaluation of the First 18-Inch Part

The first part (Fig. 20) had good surface definition. The radii were well defined and the hat web/skin intersection was dense, having been filled with unidirectional fibers over the full length of the part.

Additional 18-Inch Parts

Several other 18-inch parts were made with only minor changes to the manufacturing plan. Fig. 21 shows one part that was made and then cut into 16 divisions to check the wall thickness dimensions. Fig. 22 shows the recorded measurements. Fig. 23 shows an 18-inch part where the intersection of the hat and skin plies were sewn in two parallel rows on each side of the hat stiffener. Fig 24 shows a part where two hat sections were cocured to a wide skin layup.

Fabrication Plan for a Full-Scale 18-Foot Part

Manufacturing sequence number 3 (Fig. 13) was employed in the manufacture of the 18-foot part. The major change in this sequence plan was the fabrication of a more durable, but still flexible, overpress tool in which the hat-section layups were made. This tool is now the major tool in the manufacturing sequence. Test sample work had been done on the woven graphite-epoxy material including dielectric monitored cure cycle evaluations. The only foreseeable problem would be a result of scale-up.

Tooling and Tool Fabrication for 18-Foot Part

The skin layup tool (Fig. 25) was fabricated from ½-inch thick aluminum plate stock, 10 inches wide and 20 feet long. Three plates were welded to form a "U"-shaped tool. The two legs of the tool were cross-braced at the ends and at two other locations equally spaced from each other. The tool was then rotated 180 degrees and the welded edges beveled to break the sharp edges. All surfaces of the tool were coated three times with a parting agent followed by light buffing of the top surface of the tool where the skin plies were to be layed up.

A high-temperature glass/epoxy laminate for the overpress layup forming tool was made over a 22-foot plaster edge-run pattern as shown in Fig. 26. The plaster pattern was dried and coated with a lacquer-sealer, air dried, and then coated with a standard

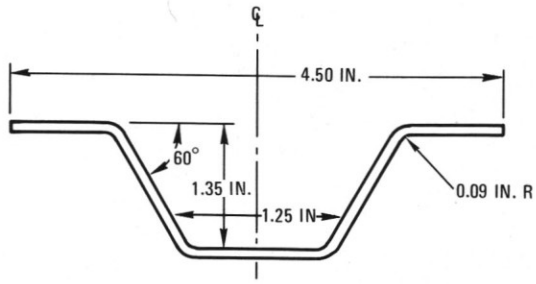

Fig. 18 Formed aluminum overpress tool.

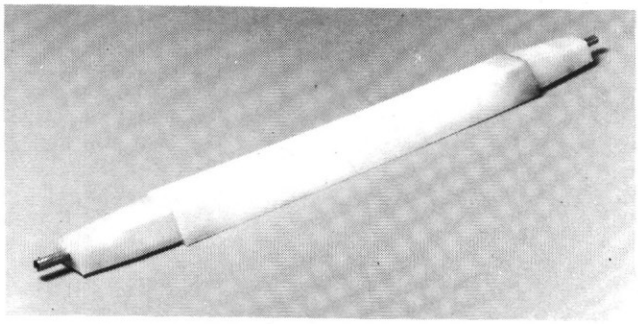

Fig. 19 Completed inflatable rubber mandrel.

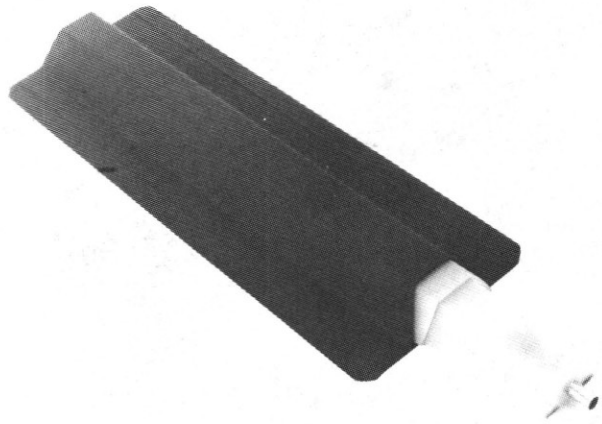

Fig. 20 Completed hat/skin part number 1.

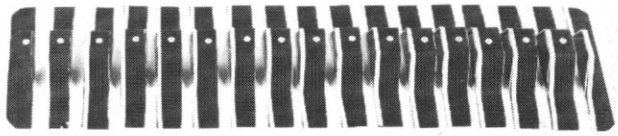

Fig. 21 Part number 2 sectioned for thickness measurements.

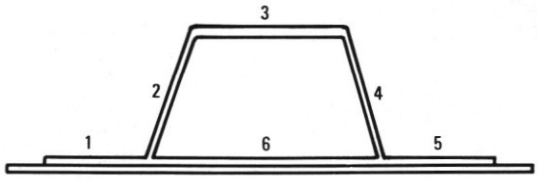

AREA	CROSS SECTION LOCATION					
	1	2	3	4	5	6
A	0.0460	0.0255	0.0538	0.0250	0.045	0.0390
B	0.0470	0.0253	0.0535	0.0250	0.0445	0.0390
C	0.047	0.0250	0.0535	0.0250	0.0465	0.0395
D	0.047	0.0250	0.0540	0.0250	0.0470	0.0390
E	0.047	0.0250	0.0540	0.0250	0.0460	0.0395
F	0.047	0.0250	0.0530	0.0250	0.0470	0.0395
G	0.0475	0.0250	0.0540	0.0255	0.0470	0.0395
H	0.047	0.0250	0.0540	0.0250	0.0465	0.0395
I	0.047	0.0250	0.0545	0.0250	0.047	0.0390
J	0.0475	0.0250	0.0545	0.0250	0.0465	0.0390
K	0.047	0.0250	0.0545	0.0255	0.0465	0.0390
L	0.047	0.0255	0.0545	0.0255	0.0470	0.0390
M	0.0465	0.0250	0.0545	0.0255	0.0465	0.0390
N	0.047	0.0250	0.0540	0.0255	0.0470	0.0390
O	0.0465	0.0250	0.0545	0.0255	0.0470	0.0390
P	0.047	0.0255	0.0540	0.0250	0.0465	0.0390

Fig. 22 Wall thickness measurements of part number 2.

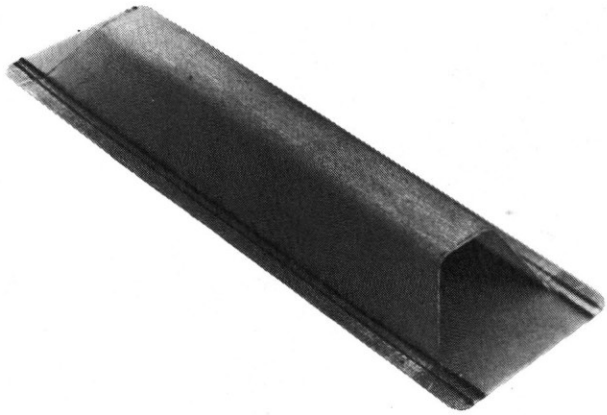

Fig. 23 18-inch, development part with sewn outer flanges.

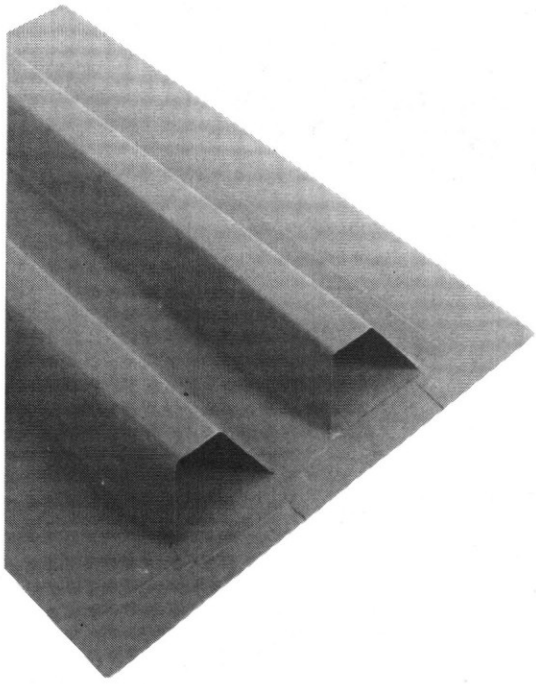

Fig. 24 Double 18-inch part.

shop-type film parting agent prior to installing the epoxy laminate layup. The 20-foot glass-epoxy overpress tool was laminated in stages to a thickness of 3/8 inch.

It was decided to incorporate an extruded rather than molded silicon rubber mandrel into the program because it would more nearly represent the production circumstance. A different chemical formulation (D-Aircraft Corporation extrudable rubber formulation D-650) was used. This was done to stiffen the mandrel wall without increasing the thickness. In fact, the thickness was reduced from 0.125 to 0.10-inch. It was believed that a thinner-wall mandrel might greatly improve the pull-out operation. However, as the thickness of the wall decreases, the more the mandrel must be internally stiffened during the layup stages to support the mandrel layup wrapping operation. A removable wooden mandrel insert was used to support the rubber mandrel during layup. The wooden support was removed prior to vacuum bagging the entire assembly for an autoclave heat and pressure cure.

18-Foot Part Fabrication

The design/analysis study indicated a hat-web angle (α) change from 30 to 15 degrees prior to a more thorough study

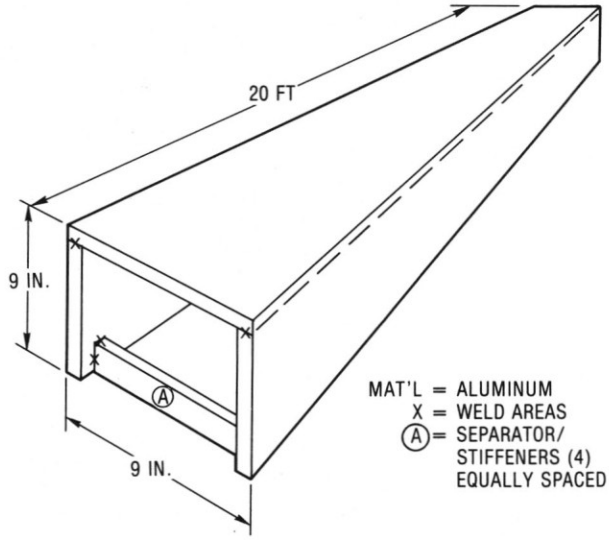

Fig. 25 Eighteen foot-long hat/skin part layup tool.

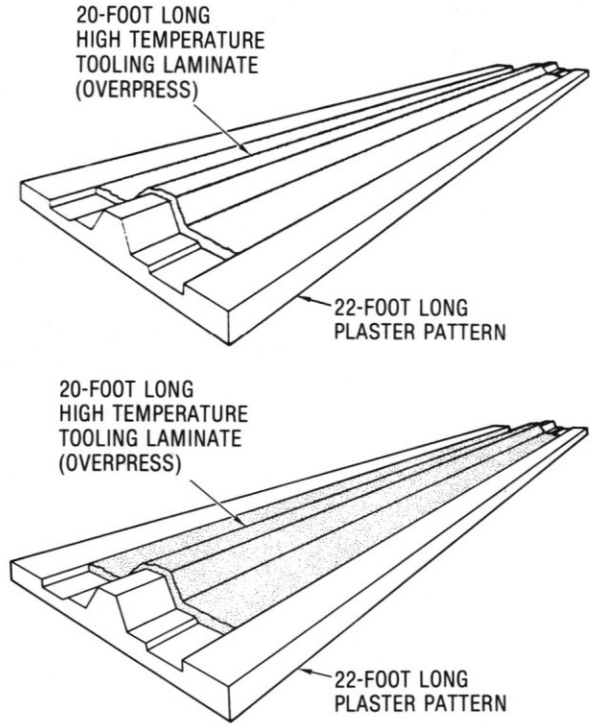

Fig. 26 High-temperature laminated overpress tool.

which later optimized the web angle at zero degrees, or perpendicular to the skin surface. Fig. 1 shows the 15-degree angle design. Also at this time, the hat/web and hat/crown thicknesses were made equal. All full-scale 18-foot parts used this intermediate design. Also, although the design was based on unidirectional fiber studies, the substitution of woven fabric was not considered a major problem, mainly due to the ply orientations of the recommended layup.

Skin layup consisted of four plies laid at (+45/0/90/-45) degrees on the layup tool with the zero fiber direction established by the warp direction of the fabric. Skin width was set at nine inches and the length at 18 feet. The hat stiffener consisted of six plies of woven fabric layed up in $(40\text{-}0\text{-}90)_S$ sequence. No special fabric compacting methods were used. The material was stacked using a Teflon squeegee to wipe each ply against the previous ply

layup. The skin was layed up over one ply of Style 120 Teflon impregnated glass fabric parting fabric (Armalon). The Armalon was taped to the surface of the tool.

The first step in the layup of the hat section was the application of the Frekote-44 parting agent to the inflatable rubber mandrel. This was accomplished by three air-dried coats of parting agent without any buffing of the surface of the rubber. The removable wooden support tool mandrel was then placed into the rubber mandrel and set aside while flat layups for the hat-section were prepared. The flat hat-section plies were then layed over the mandrel, inverted, and placed firmly in the overpress tool. Next, the three inboard web plies were wrapped tightly around the mandrel assembly and the outboard web plies were formed against the overpress tool. The entire overpress assembly was then placed in position over the skin layup.

The only bleeder involved in the layup assembly was the Armalon between the overpress and the hat layup. The equivalent of four plies of Style 181 glass bleeder fabric was placed around all edges of the laminated assembly, but not touching the layup. Also, there was no bleeder placed over the overpress.

The assembly was then vacuum bagged for an autoclave cure. A dielectric monitor probe was placed at one end of the layup and three thermocouples were used; one at each end, and one in the middle of the aluminum layup and cure tool. Small holes were drilled into the tool close to the vacuum edge and the thermocouple sensor ends firmly pressed into the holes and then covered with sealant tape. The ends of the rubber mandrel were left open without any 3/8-inch tubes protruding as previously done on the 18-inch parts, and the vacuum bag was attached to the mandrel by vacuum sealant tape plus a thin roll of uncured silicone rubber.

The completed assembly was placed in the autoclave with the dielectric monitor probes positioned nearest the door of the autoclave. The entire length of the assembly was then covered with a woven glass fabric insulation blanket (four plies of 181 glass fabric and two plies of Airweave synthetic bleeder material). Four additional heavier plies of glass fabric were wrapped around the forward end of the assembly. The cure cycle consisted of a rapid heatup rate to 200F followed by a hold at this temperature until all three thermocouples were within 10F. The temperature was then raised to 350F. The temperature rise rate, as well as the pressure (100 psi) application point, were dictated by the dielectric monitor.

Part Removal

The 18-foot part was easily removed from the overpress and the layup-and-cure tool. The inflatable rubber mandrel initially required about a 100-pound pull force to shrink the rubber mandrel sufficiently away from the sides of the graphite-epoxy part. Once the intimate contact areas were parted, about a 25-lb pull was all that was required to continually move the mandrel out. Also, when the end of the mandrel reached the half-way point, the removal force diminished until a gentle pulling force was all that was required to completely remove the rubber mandrel from the part.

Part Evaluation

The 18-foot full-scale component (Fig. 27) was evaluated for:

1. Additional changes to the manufacturing plan.
2. Ease of part removal from the layup and cure tools.
3. Ease of rubber mandrel removed from the internal area of the 18-foot part.
4. Degree of cleanup required prior to layup of an additional full-scale part.
5. Visual acceptance.
6. Cross-sectional integrity along the length of the 18-foot part.

Visually, the section cuts from the part were of high quality. The part appeared to be dense and all of the radii, though not to design specification (0.060 inch), were crisp and clean. The edges of the hat-stiffener webs, where they merged into the skin, and the inside fabric overlap at the base of the hat-section, were also well blended.

Fig. 28 shows a cross-sectional view and three photos taken from encapsulated micrograph specimens at various levels of magnification. The void area at the hat-section web flange dividing point was caused by not filling that area with unidirectional or other fillers prior to cure. It extended along the full length of the 18-foot part. Consideration had been given to filling these areas with unidirectional fibers as other aerospace companies had done, but we were more interested on the first part in determining how well an inflatable rubber mandrel could form the internal side walls against the overpress tool and into the radii; and if unsuccessful, fiber filling was a known technique. The resin and fiber content by weight of the 18-foot part was 30.5 percent and 69.5 percent respectively. Voids were less than one percent of total volume, with the exception of the flange/skin intersection point.

IV Conclusions

Flat- and curved-crown concepts of graphite-epoxy tape, hat-stiffened panels were included in a design/analysis study that included many cases of varying configuration and ply-stacking sequences. The analysis was performed by use of the STAGSC computer code, wherein bifurcation buckling results were employed in a qualitative manner for determining relative efficiencies between cases for the two concepts involved. Further

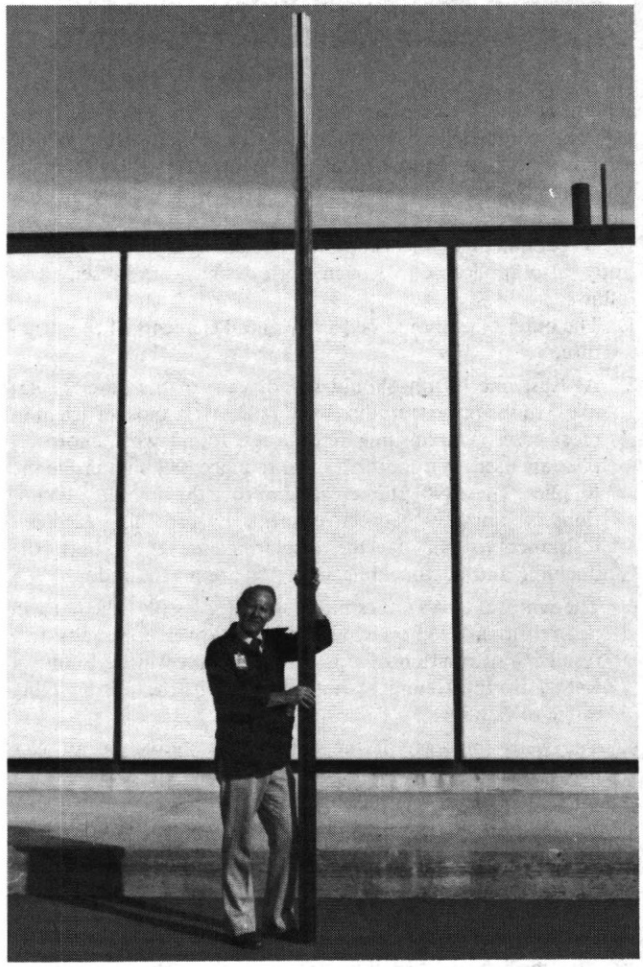

Fig. 27 Full-scale, 18-foot, composite hat/skin component.

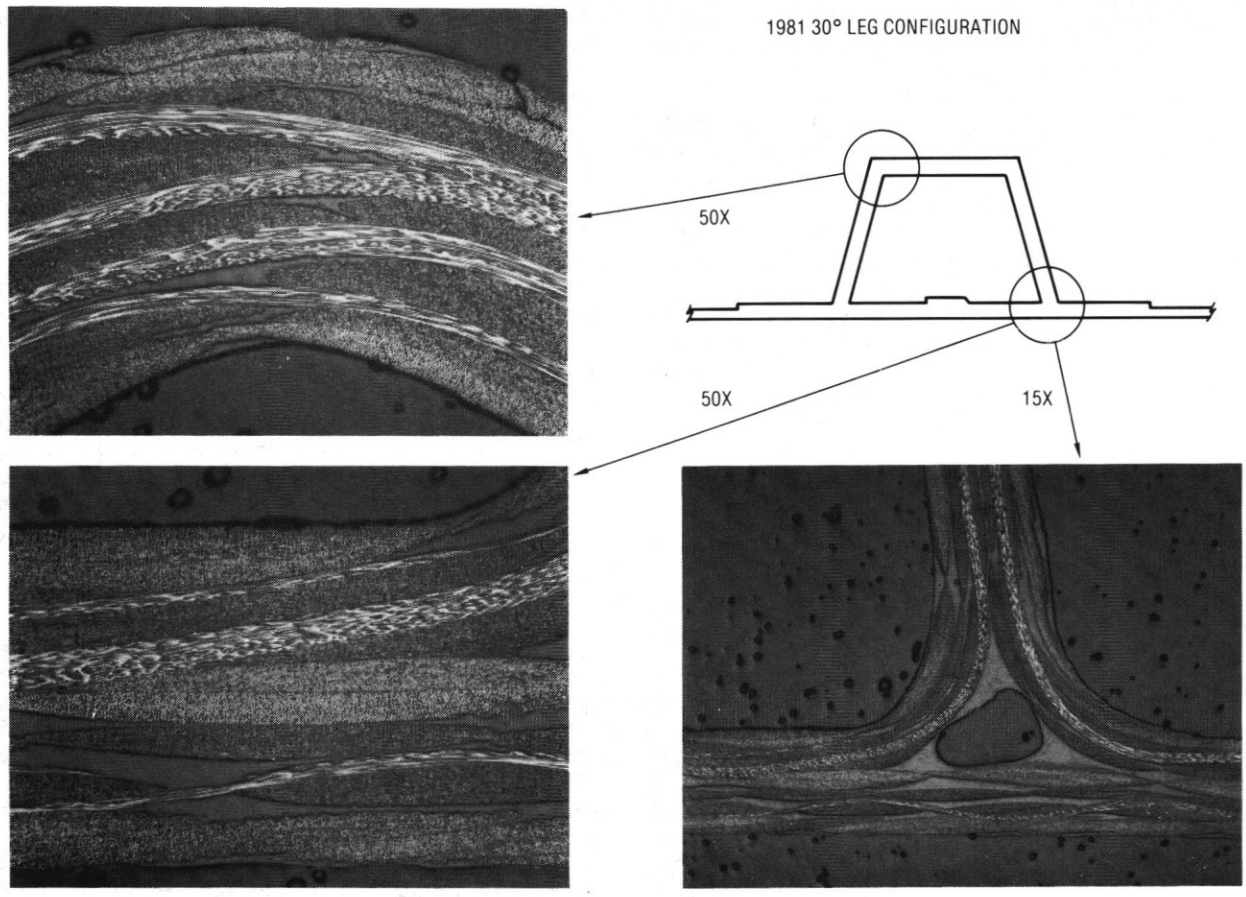

Fig. 28 Specimen sectioned from 18-foot, full-scale hat/skin part.

analysis is needed where woven graphite-epoxy cloth, either partially or completely, is included in the panels, this will be necessary so that tradeoffs can be accommodated with automated manufacturing problems associated with the use of both tape and woven cloth.

Predominant conclusions based on the design/analysis study, also applicable to woven cloth designs, are presented as follows:

1. The outer plies should be [±45] for all elements of the structure.
2. At least one [0] ply should be adjacent to the outer [±45] plies. In the present study, two [0] plies were most efficient in most cases. Diminishing returns are found when more [0] plies are used. It is more efficient to place [90] plies inside the [0] plies. These [90] plies greatly improve the boundary conditions at junctures between elements by providing excellent resistance to out-of-plane displacements; thus, both the buckling and postbuckling strengths are maximized.
3. The removal of any plies in the webs (or legs) of the hat will not result in weight savings; in fact, a weight penalty will result. Confirmation of this determination will be found in Ref. 7 by the testing of hat stiffeners in the postbuckling range to failure.
4. The webs (or legs) of the hat section should be as near perpendicular to the skin as possible (some draft is required for part removal from tooling after cure).
5. The strength to weight ratios of the curved-crown hats are considerably greater than those of the flat-crown hats.

Results of the manufacturing study provide some of the answers to the key issues governing the development of cost-effective mechanized techniques for quantity production of advanced composite aircraft structure. The manufacturing approaches taken during this work, though unique and often quite bold, are now considered valid. Specifically, we have successfully demonstrated:

1. Elimination of excess bleeder fabric from the layup; edge bleeding alone is sufficient.
2. Elimination of precompaction of resin-impregnated fabric to bring resin content to about 30% during heat curing operations.
3. Thin-walled (less than 0.10-inch) elastomeric rubber internal hat-section mandrels performed the best of those evaluated to date. They are easily withdrawn from the hat-section (especially when vacuum is applied to overcome the surface adhesion between the laminate and the mandrel), and they provide adequate equalized pressure for forcing the layup solidly against a rigid backup tool.
4. Resin cleanup is minimized by the use of a permanent Teflon film or fabric coating applied to all tools that contact the layup during the heat and pressure cure.
5. Excessive resin bleeding during cure is not required to produce acceptable parts.
6. The total tooling/process approach is valid. Acceptable quality (structural integrity) parts have been fabricated.
7. Major layup problems were not encountered in using the woven graphite material. The manufacturing sequence can be modified to facilitate mechanized layup. The use of tape will be ascertained at a later date.
8. The manufacturing layup configuration was reduced from the multi-step process shown in Fig. 29 to the more simplified and readily adaptable to mechanization concept shown in Figs. 13 and 30.

It is anticipated that the curved-crown hat concept would have less manufacturing problems.

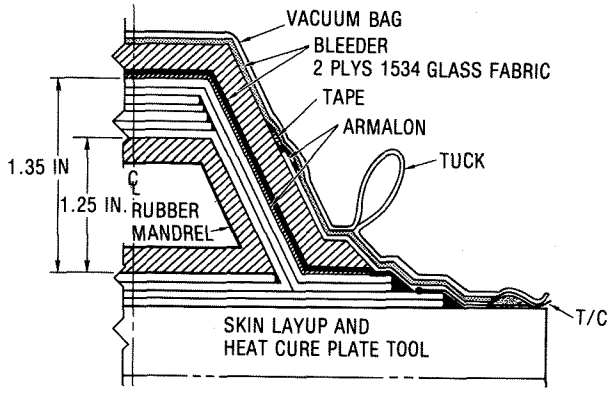

Fig. 29 Manufacturing sequence number 1 layup.

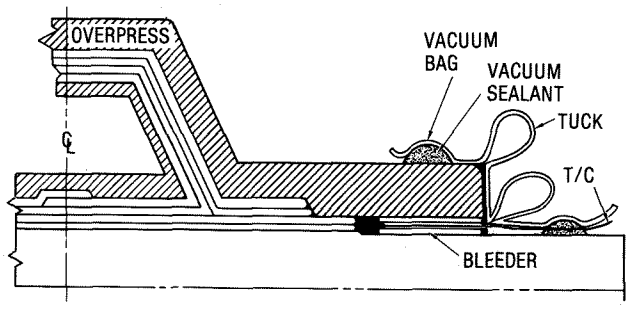

Fig. 30 Manufacturing sequence number 3 layup.

1. Spier, E.E., *On Experimental Versus Theoretical Incipient Buckling of Narrow Graphite/Epoxy Plates in Compression* AIAA-80-0686 paper published in Proceedings of AIAA/ASME/ASCE/AHS 21st Structures, Structural Dynamics & Materials Conference May 12-14, 1980, pp 187-193.
2. Spier, E.E., *Stability of Graphite/Epoxy Structures with Arbitrary Symmetrical Laminates*, Experimental Mechanics, Vol. 18, No. 11, November 1978, pp 255-271.
3. Spier, E.E. and Klouman, F.L., *Empirical Crippling Analysis of Graphite/Epoxy Laminated Plates,* Composite Materials: Testing & Design (4th Conference), ASTM STP 617, 1977, pp 255-271.
4. Gerard, G., *Introduction to Structural Stability Theory*, McGraw-Hill, 1962, pp 67.
5. Almroth, B.O., et al, *Structural Analysis of General Shells, User Instructions for STAGSC*, Vol. III, Report NO. LMSC D502277, Lockheed Structural Mechanics Laboratory, Lockheed Palo Alto Research Laboratory, Palo Alto, California, December 1975.
6. Spier, E.E. and Klouman, F.L., *Postbuckling Behavior of Graphite/Epoxy Laminated Plates and Channels,* 1976, Army Symposium on Solid Mechanics, Composite Materials: The Influence on Mechanics of Failure on Design, Cape Cod, Mass., September 1976, pp 62-78.
7. Spier, E.E., *Postbuckling Fatigue Behavior of Graphite-Epoxy Stiffeners,* AIAA-82-0779 paper, published in Proceedings of AIAA/ASME/ASCE/AHS 23rd Structures, Structural Dynamics & Materials Conference, May 10-12 1982, pp 511-527.